4.2.3 Spherical SWE in 1D

We also consider the spherical shallow water equations in a 1D setting, focusing on the linearized SWE on a circular domain. The length of the domain corresponds to the circumreference of the circle, $L = 2\pi$, and is discretized into $N = 500$ points. The initial conditions is specified as a Gaussian function wrapped around the circle, expressed as:

$$h(\theta, 0) = h_0 \exp\left(\frac{-(\theta - \mu)^2}{2\sigma^2}\right),$$

where the parameters are $h_0 = 1, \mu = \frac{\pi}{4}, \sigma = \frac{\pi}{16}$. The initial conditions can be seen in Figure 4.26.

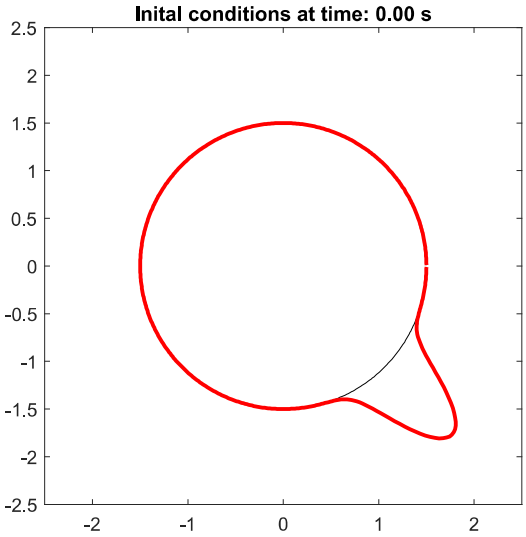

Figure 4.26: Initial conditions for the 1D linearized shallow water equations in spherical coordinates.

The numerical solution in the θ, t plane is shown in Figure 4.27, for $t = 0$ to $t = 1$.

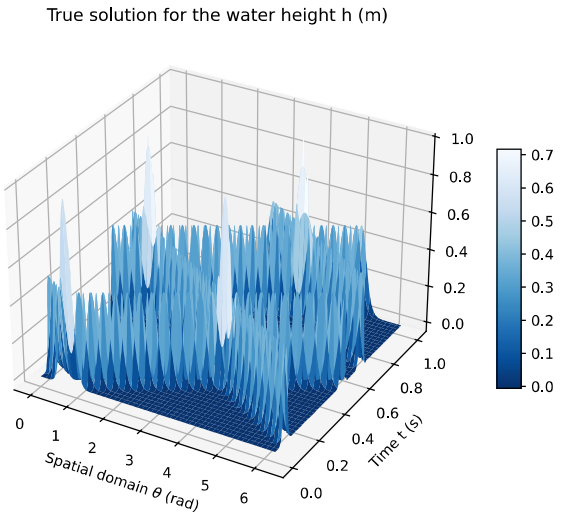

Figure 4.27: Numerical solution of the spherical shallow water equations in 1D in the $\theta, t-$space.

Based on the data generated by the numerical solution (we use time steps of $\Delta t = 0.0025$), we train a FNO model and a Convolutional Neural Network (CNN) model.

FNO

The FNO model consists of an input channel, 64 hidden channels and an output channel. We use a Fourier basis with 16 modes and a batch size of 32. The model is trained using the Adam optimizer with a learning rate of 0.001, a total of 100 epochs and the critera is to minimize the mean squared error (MSE). The model is trained on the data from $t = 0$ to $t = 0.6$, validated on the data from $t = 0.6$ to $t = 0.8$, and tested on the data from $t = 0.8$ to $t = 1.0$. The training and validation loss is shown in Figure 4.28.

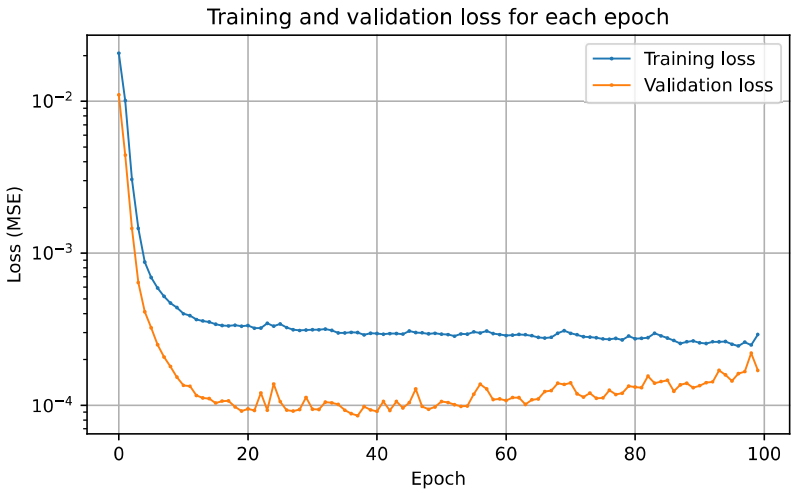

Figure 4.28: Training and validation loss for the FNO model for the spherical shallow water equations in 1D.

From Figure 4.28 we see that the model is able to learn the dynamics of the solution, but the validation loss is increasing after a certain number of epochs. The error plots are shown in Figure 4.29.

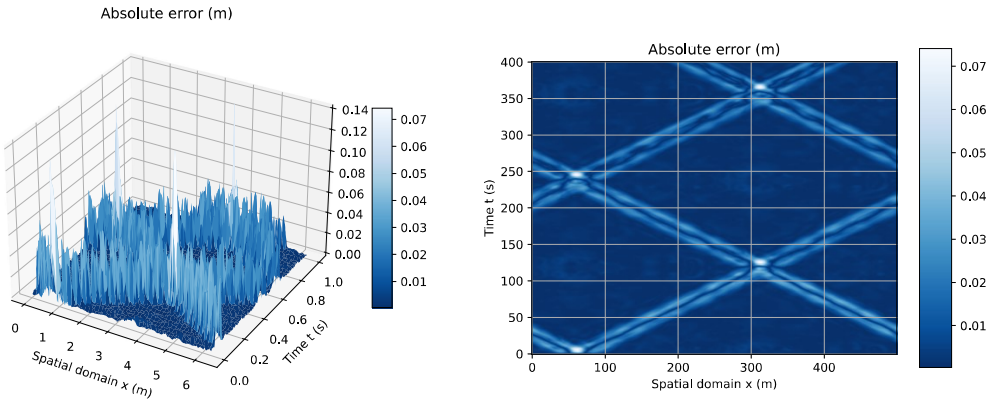

Figure 4.29: Error plots for the predictions of the 1D linearized spherical SWE.

From Figure 4.33 we see that the model is able to learn the dynamics of the solution. We also see that the absolute error is biggest at the edges of the solution, which is expected, as the solution tends to be discontinuous. To get an overview of the performance of the model, we consider the predictions for some given time steps, shown in Figure 4.30.

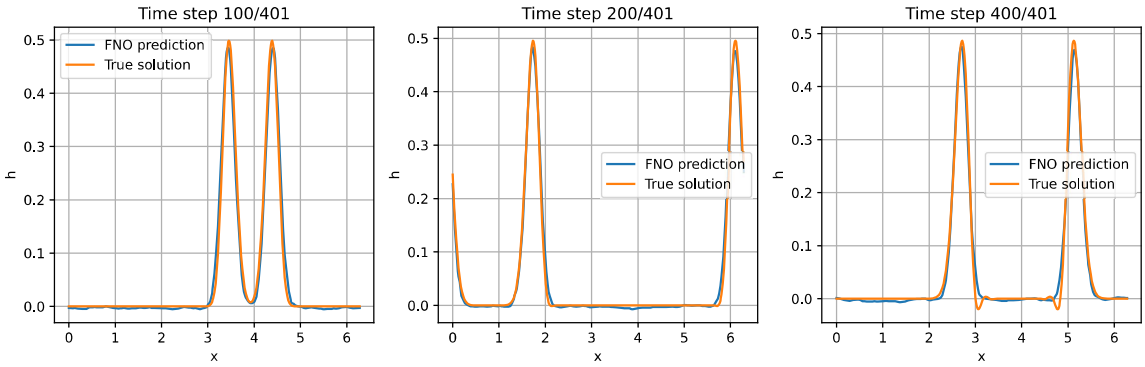

Figure 4.30: Predictions for the spherical shallow water equations in 1D.

From Figure 4.30 we see that the FNO predictions are smooth and rather accurate, but have some small errors in the top of the waves. Finally we consider the RMSE for the predictions, shown in Figure 4.31.

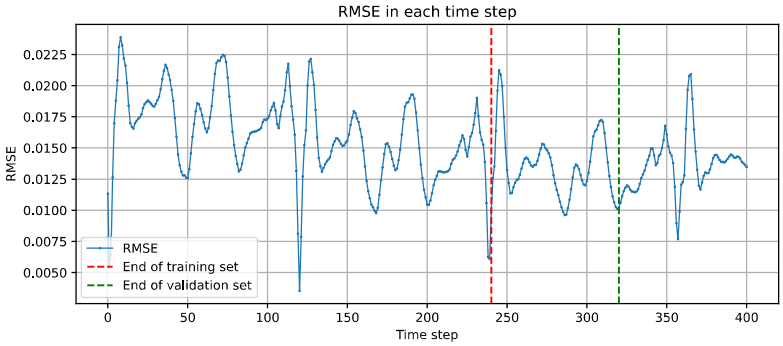

Figure 4.31: RMSE for the predictions for the spherical shallow water equations in 1D.

From Figure 4.31 we see that the RMSE is not increasing for the predictions, which is a good sign.

CNN

We have also trained a CNN model on the data generated by the numerical solution of the SWE in 1D. Like the FNO model, the CNN model is trained on the data from $t = 0$ to $t = 0.6$, validated on the data from $t = 0.6$ to $t = 0.8$, and tested on the data from $t = 0.8$ to $t = 1.0$. The training and validation loss is shown in Figure 4.32.

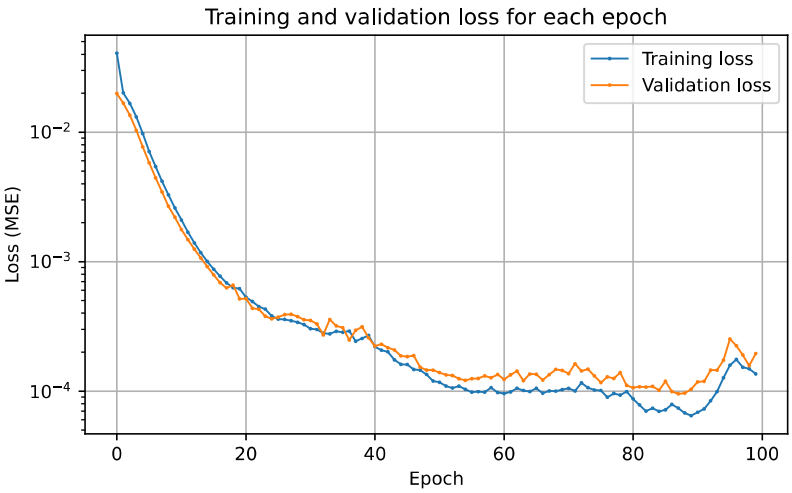

Figure 4.32: Training and validation loss for the CNN model for the spherical shallow water equations in 1D.

The error plots for the predictions of the CNN model are shown in Figure 4.33.

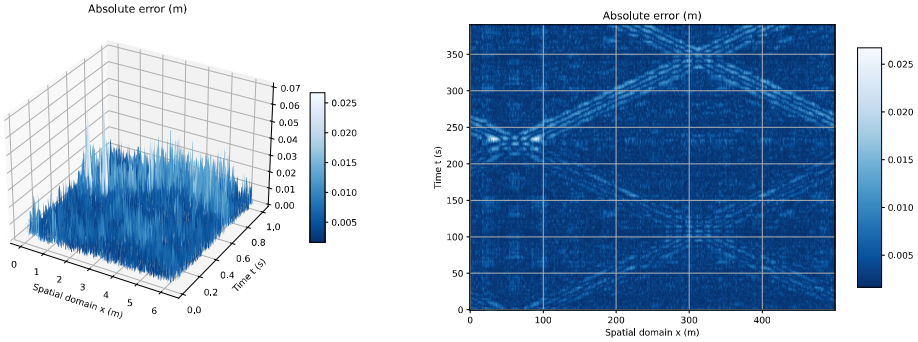

Figure 4.33: Error plots for the predictions of the CNN model for solving the 1D linearized spherical SWE.

From Figure 4.33 we see that for the CNN model, the errors are more noisy than for the FNO model. The predictions for some given time steps are shown in Figure 4.34.

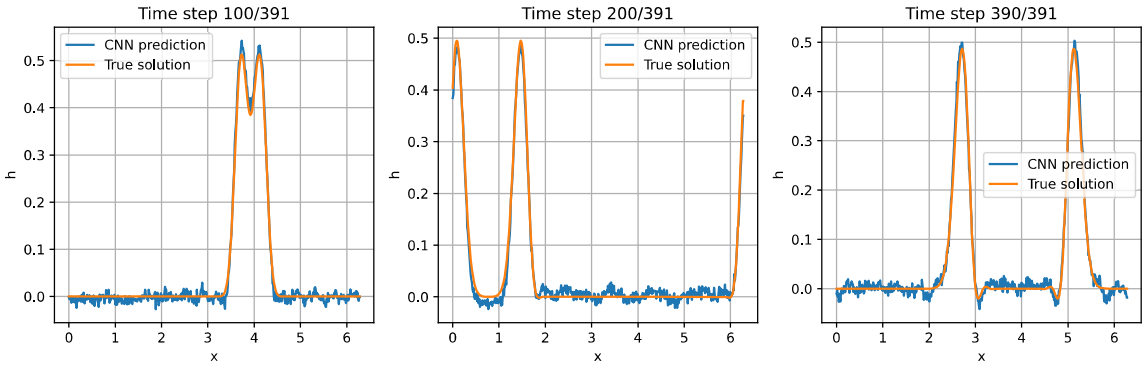

Figure 4.34: Predictions for the spherical shallow water equations in 1D using the CNN model for some given time steps.

From Figure 4.34, we also see that the predictions capture the waves, but are more noisy than the FNO predictions. Finally we consider the RMSE for the predictions, shown in Figure 4.35.

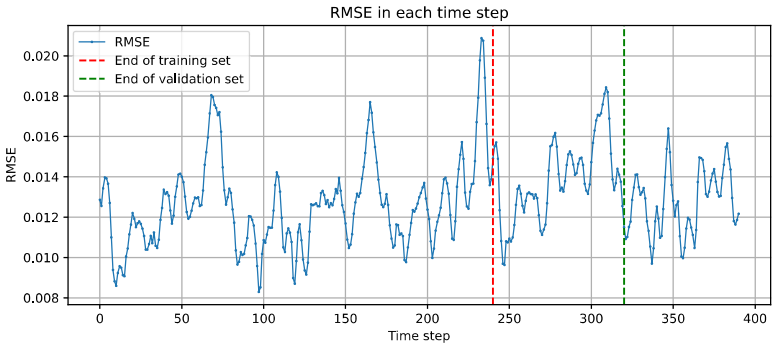

Figure 4.35: RMSE for the predictions for the spherical shallow water equations in 1D using the CNN model.

To get an overview of the performance of the different models, we consider the MSE for the predictions for the 1D SWE spherical case.

Model	$\sigma = \pi/8$			$\sigma = \pi/16$			$\sigma = \pi/32$		
	MSE	MAE	Time (s)	MSE	MAE	Time (s)	MSE	MAE	Time (s)
CNN	6.72e-05	6.48e-03	93.71	1.35e-04	8.40e-03	98.77	3.06e-04	1.25e-02	96.53
FNO	2.25e-04	9.78e-03	133.87	1.47e-04	7.12e-03	109.65	4.44e-04	1.07e-02	108.69

Table 4.3: Test loss in terms of MSE and MAE, and time for training the models for the 1D spherical SWE.

From Table 4.3 we see that the CNN model is slightly faster and better than the FNO model for $\sigma = \pi/8$ and $\sigma = \pi/16$, but for $\sigma = \pi/32$, the performance of the CNN model is decreasing. Probably due to the fact that the smaller the σ, the more discontinuous the solution is, and the FNO model is better at capturing the discontinuities. We see that the MAE in general is higher than the MSE, and is also increasing for smaller σ. Additionally, we observe that the MAE is higher, as it places more weight on small errors compared to the MSE. And in the CNN case we see a lot of small errors/noise, which is why the MAE is higher than the MSE.